

## Fuzzy Sliding Mode Control for DFIG-based Wind Energy Conversion Optimization

Han Yaozhen<sup>\*1,2</sup>, Liu Xiangjie<sup>1</sup>

<sup>1</sup>School of Control and Computer Engineering, North China Electric Power University, Beijing, China

<sup>2</sup>School of Information Science and Electrical Engineering, Shandong Jiaotong University, Jinan, China

\*Corresponding author, e-mail: hyz125@163.com

### Abstract

*This study proposes a fuzzy sliding mode control strategy to realize wind energy conversion optimization based on doubly-fed induction generator (DFIG). Its operational points in partial load zone can be electronically controlled. Chattering in wind energy conversion sliding mode control system is greatly alleviated based on fuzzy switching gain adjustment. The purposes including the maximum power point tracking, decoupling control of active and reactive power of fed induction generation system are fulfilled. Fitful and random wind speeds are mathematical modeled. Simulation results verified effectiveness and feasibility of the proposed control strategy under the two types of wind speed and indicate that the whole control system has better robustness against uncertainties and can guarantee the power quality.*

**Keywords:** DFIG, wind energy conversion optimization, sliding mode, fuzzy gain adjustment

**Copyright © 2014 Institute of Advanced Engineering and Science. All rights reserved.**

### 1. Introduction

The increasing energy demand, together with the harmful effect of fossil fuel exploitation on the climate and environment, are among the main factors that have boosted worldwide interest in renewable energies. Among a variety of renewable-energy resources, wind power is drawing the most attention from all over the world. Under an advanced wind energy growth projection, coupled with ambitious energy saving, wind power could be supplying 29.1% of the world electricity by 2030 [1]. On account of the distinct advantages, including flexible power control, competitive durability, and low converter volume, DFIGs have been widely applied in the wind-turbine generation systems, compared with other solutions such as fixed-speed induction generators or the ones with fully rated converters [2].

Now the most hot contents about wind energy conversion system (WECS) under research are [3] the innovation on the generator, drive train and power electronics, the research for new materials and designs for the wind turbines, the use of signal observation theory to estimate parameters or variables of interest, and the development and design of novel control strategies.

The main control objective of variable speed WECS is power extraction maximization. For realizing this goal, the so-called turbine tip speed ratio should be maintained at its optimum value in despite of wind variations. Nevertheless, control is not always aimed at capturing as much energy as possible. In fact, in previously rated wind speed, the captured power needs to be limited. Although there are both mechanical and electrical constraints, the more severe problems are commonly on the generator and the converter. Therefore, regulation of the power produced by the generator is usually considered. Sliding mode controller with interesting characteristics make it attractive to deal with these kinds of system, which rely on a random source as the wind, have nonlinear behavior and operate under external disturbances and uncertainties in the model parameters [4-5]. Higher order sliding mode algorithms are even used which have achieved outstanding control effects [6-7]. However, in standard sliding mode there are larger chattering and for higher order sliding mode mass complicated parameters are needed calculated offline.

A fuzzy sliding mode controller for a wind power system with a twofold objectives, stator reactive power regulation to compensate the grid power factor, and maximize the extracted power by tracking a torque reference to control the points of operation within the partial load

zone is designed in this paper. The proposed control scheme provide a suitable compromise between simplicity and robustness, drive train mechanical stresses and conversion efficiency.

## 2. WECS Model

### 2.1. Analysis of Wind Turbine Characteristic

This paper concentrate on grid-connected WECS with slip power recovery whose configuration can operate at different speeds but generates electricity at the constant frequency and voltage fixed by the grid and, adequately controlled, allows power conversion maximization and mechanical stress alleviation. Specially a simple topology has been selected as a case of study. A schematic diagram of this configuration is shown in Figure 1.

As it can be observed, both stator and rotor circuits provide power to the grid, delivering thus more power than the rated and increasing the efficiency. The power is directly delivered from the stator side and through a bidirectional converter from the rotor side. The converter consists of an uncontrolled bridge rectifier, a smoothing reactor, and a line-commutated inverter, whose firing angle can be modified to control the generator torque and, hence, the system operation speed and the operation point.

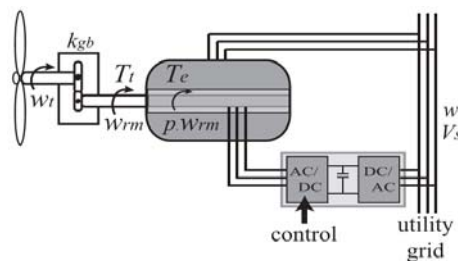


Figure 1. WECS-DFIG Configuration

In fact, the mechanical power that a wind turbine can capture is less than the available power in the wind and it can be written as:

$$P_t = 0.5\pi\rho B_l^2 C_p(\lambda, \beta_p) v^3 \quad (1)$$

Where  $\rho$  is the air density,  $v$  represents the wind speed,  $B_l$  is the blade length, and  $C_p$  is the power coefficient of the turbine, which depends on the shape and the geometry of the blades. This coefficient is a nonlinear function of the pitch angle of the blades  $\beta_p$ , and the tip speed ratio,  $\lambda = \omega_{rm} B_l / k_{gb} v$ , where  $\omega_{rm}$  is the mechanical rotation speed of the generator rotor and  $k_{gb}$  the gear box relation. When the pitch angle is maintained fixed, the  $C_p(\lambda) = c_1(c_2/\lambda - 1)e^{-c_3/\lambda}$  has a unique maximum, for  $\lambda = \lambda_{opt}$  as it can be seen in Figure 2.

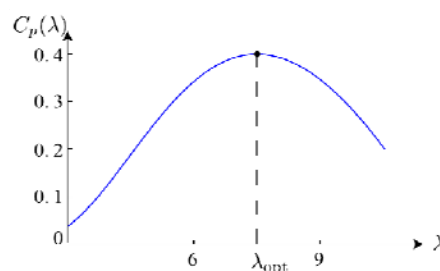


Figure 2. Power Coefficient  $C_p(\lambda)$

As is indicated in Figure 3, with respect to power generation, two regions can be distinguished in the useful operation range of the turbine. Within the partial load zone, that is between  $v_{cut-in}$  (minimum wind speed at which the turbine starts generating) and the rated speed  $v_{rated}$ , it is desirable to maximize the extraction of the energy available in the wind. The control in this zone is usually performed electronically, maintaining the pitch angle fixed. The other useful region, known as the full load zone, is defined between  $v_{rated}$  and  $v_{cut-out}$  (limit wind speed, up from which the turbine should be turned off to prevent damages). Within this zone the extraction of power is limited to the rated value, which can be accomplished by controlling either the pitch angle of the blades or the electrical variables of the DFIG[8]. The study in this paper concentrates on the partial load zone.

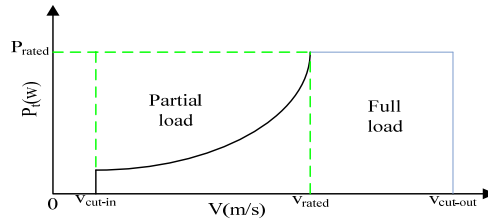


Figure 3. Wind Turbine Operation Zone

## 2.2. Reduced Dynamic Model

The DFIG model is a multivariable, nonlinear and strong coupling system under three phase stationary coordinate framework. In order to adjust active and reactive power independently, the generator model under the two phase rotating coordinate is deduced [9].

Voltage mathematical equation is:

$$\begin{cases} u_{ds} = R_s i_{ds} + \dot{\phi}_{ds} - \omega_s \phi_{qs} \\ u_{qs} = R_s i_{qs} + \dot{\phi}_{qs} + \omega_s \phi_{ds} \\ u_{dr} = R_r i_{dr} + \dot{\phi}_{dr} - (\omega_s - p\omega_{rm}) \phi_{qr} \\ u_{qr} = R_r i_{qr} + \dot{\phi}_{qr} + (\omega_s - p\omega_{rm}) \phi_{dr} \end{cases} \quad (2)$$

Flux linkage is:

$$\begin{cases} \phi_{ds} = L_s i_{ds} + L_m i_{dr} \\ \phi_{qs} = L_s i_{qs} + L_m i_{qr} \\ \phi_{dr} = L_r i_{dr} + L_m i_{ds} \\ \phi_{qr} = L_r i_{qr} + L_m i_{qs} \end{cases} \quad (3)$$

Where the variables  $u$   $i$   $R$   $\phi$  represent voltage, current, electric resistance and flux. Subscripts  $s$   $r$   $d$   $q$  represent the stator and rotor component, quadrature components, Moreover,  $\omega_s$  is the frequency of the grid (in rad/s),  $p$  is the number of pole pairs,  $L_s$  and  $L_r$  are the self-inductances of the windings, and  $L_m$  is the mutual inductance between windings.

The last equation accounts for the mechanical dynamics of the rotating parts, which can be denoted by:

$$\dot{\omega}_{rm} = \frac{1}{J} (T_t - T_e) \quad (4)$$

Where  $J$  represents the inertia of the whole rotating parts,  $T_e$  is the electrical resistant torque of the DFIG, and  $T_t$  is the torque produced by the wind on the blades (referred to the high speed shaft with the help of the gear box relation constant). these torques can be indicated as:

$$T_e = 1.5 p L_m (i_{qs} i_{dr} - i_{ds} i_{qr}) \quad (5)$$

$$T_t = \frac{\pi \rho B_i^3 C_t(\lambda) v^2}{2 k_{gb}} \quad (6)$$

Where  $C_t(\lambda)$  is the torque coefficient of the turbine, defined as  $C_p(\lambda)/\lambda$ .

The WECS described previously can be simplified by making some electrical and geometrical considerations, regarding the relative alignment between the rotating frames and the spatial fluxes, and neglecting the stator resistance, A 3-order model which is adequate for the control design process can be deduced [10]. This description consists of three differential equations accounting for electrical dynamics of the rotor and the dynamics of the mechanical rotational speed.

$$\begin{cases} \dot{i}_{qr} = - \left( \frac{L_m U_s}{L_e} + \omega_s i_{dr} \right) (1 - p \omega_{rm} / \omega_s) - \frac{R_r L_s}{L_e} i_{qr} + \frac{L_s}{L_e} u_{qr} \\ \dot{i}_{dr} = \omega_s i_{qr} (1 - p \omega_{rm} / \omega_s) - \frac{R_r L_s}{L_e} i_{dr} + \frac{L_s}{L_e} u_{dr} \\ \dot{\omega}_{rm} = \frac{1}{J} \left( T_t(v, \omega_{rm}) - \frac{3 p L_m U_s}{2 \omega_s L_s} i_{qr} \right) \end{cases} \quad (7)$$

Where  $U_s$  is the grid line voltage and  $L_e = L_s L_r - L_m^2$ . The stator currents can be algebraically calculated knowing the rotor currents.

$$\begin{cases} i_{qs} = - \frac{L_m}{L_s} i_{qr} \\ i_{ds} = \frac{U_s}{\omega_s L_s} - \frac{L_m}{L_s} i_{dr} \end{cases} \quad (8)$$

When the generator is operating on the points where the power extraction is maximum ( $C_p = C_{p\max}$ ,  $\lambda = \lambda_{opt}$ ), the corresponding torque can be expressed as a function of the squared rotational speed.

$$T_{opt}(\omega_{rm}) = \frac{\pi \rho B_i^5 C_{p\max}}{2 k_{gb}^3 \lambda_{opt}^3} \omega_{rm}^2 = k_0 \omega_{rm}^2 \quad (9)$$

Eventually, the stator reactive power can be expressed as:

$$Q_s = \frac{3 U_s^2}{2 \omega_s L_s} - \frac{3 L_m U_s}{2 L_s} i_{dr} \quad (10)$$

A proposal control strategy is designed to accomplish two simultaneous objectives simply, robustly, and avoiding unnecessary mechanical chatter. One of the aims contributes to compensate the reactive power needs of the grid, by regulating the stator reactive power following an external reference. The other involves the extraction of power controlling the points of operation so that  $T_e = T_{opt}$  for all wind speeds in the zone.

### 3. Design of Fuzzy Sliding Mode Controller for WECS

#### 3.1. Design of Sliding Mode Controller

In order to achieve the desired control objectives, the components of the sliding variables are chosen as follows:

$$s_1 = T_{ref} - T_e = T_{ref}(\omega_{rm}) - \frac{3pL_m U_s}{2\omega_s L_s} i_{qr} \quad (11)$$

$$s_2 = Q_{ref} - Q_s = Q_{ref}(t) + \frac{3L_m U_s}{2L_s} (i_{dr} - \frac{U_s}{\omega_s L_m}) \quad (12)$$

$$\dot{s}_1 = f_1(t, i_{qr}, i_{dr}, \omega_{rm}) + g_1(t, i_{qr}, i_{dr}, \omega_{rm}) u_{qr} \quad (13)$$

$$\dot{s}_2 = f_2(t, i_{qr}, i_{dr}, \omega_{rm}) + g_2(t, i_{qr}, i_{dr}, \omega_{rm}) u_{dr} \quad (14)$$

Where  $f_1(\cdot) = \frac{3pL_m U_s}{2\omega_s L_s} (\frac{L_m U_s}{L_r} + \frac{R_r L_s}{L_r} i_{qr} + (\omega_s - p\omega_{rm}) - \frac{pL_m U_s}{\omega_s L_r} \omega_{rm}) + \frac{2k_0 \omega_{rm}}{J} (T_i - T_e)$   $g_1(\cdot) = -\frac{3pU_s L_m}{2\omega_s L_r}$ ,  
 $g_2(\cdot) = \frac{3pU_s L_m}{2L_r}$ ,  $f_2(\cdot) = \dot{Q}_{ref} + \frac{3pL_m U_s}{2L_s} \left( (\omega_s - p\omega_{rm}) - \frac{R_r L_s}{L_r} i_{dr} \right)$ .

The sliding mode controller is composed by equivalent control and switching component. Effect of the former is to make the states move on the sliding manifold and the latter is to keep states not escape from sliding manifold when the system encounters uncertainties.

$$\begin{cases} u_{qr} = u_{qr}^{eq} + u_{qr}^s \\ u_{dr} = u_{dr}^{eq} + u_{dr}^s \end{cases} \quad (15)$$

Take no account of uncertainties of  $f_1, f_2, g_1, g_2$ , the equivalent control component can be get easily from  $\dot{s}_1 = \dot{s}_2 = 0$

$$\begin{cases} u_{qr}^{eq} = -g_1^{-1}(t, i_{qr}, i_{dr}, \omega_{rm}) f_1(t, i_{qr}, i_{dr}, \omega_{rm}) \\ u_{dr}^{eq} = -g_2^{-1}(t, i_{qr}, i_{dr}, \omega_{rm}) f_2(t, i_{qr}, i_{dr}, \omega_{rm}) \end{cases} \quad (16)$$

When system uncertainties exist, switching control must be employed to drive the escaped states to the sliding manifold. The switching controller is designed as (17).

$$\begin{cases} u_{qr}^s = g_1^{-1}(t, i_{qr}, i_{dr}, \omega_{rm}) K_{qr} \text{sign}(s_1) \\ u_{dr}^s = g_2^{-1}(t, i_{qr}, i_{dr}, \omega_{rm}) K_{dr} \text{sign}(s_2) \end{cases} \quad (17)$$

Where  $K_{qr} = \Delta_{qr} + \eta_{qr}$ ,  $K_{dr} = \Delta_{dr} + \eta_{dr}$ ,  $\eta_{qr} > 0$ ,  $\eta_{dr} > 0$ ,  $\Delta_{qr}, \Delta_{dr}$  are the uncertainties components such as un-modeled dynamic, parameters variation and external disturbance which are decomposes in (13), (14).

Stability analysis. The Lyapunov function is chosen as:

$$V = 0.5s_1^2 \quad (18)$$

Then,

$$\dot{V} = s_1 \dot{s}_1 = s_1 (f + \Delta_{qr} + g g^{-1}(-f - K_{qr} \text{sign}(s_1))) = s(-K_{qr} \text{sign}(s_1) + \Delta_{qr}) = -\eta_{qr} |s| \leq 0$$

The Stability proof is the same for  $s_2$ .

### 3.2. Fuzzy Switching Gain Adjustment

The chattering in (17) which is used to compensate uncertainties  $\Delta_{qr}, \Delta_{dr}$  to guarantee sliding mode existenc conditions is mainly caused by switching gains  $K_{qr}, K_{dr}$ . The chattering

can be reduced by changing  $K_{qr}$ ,  $K_{dr}$  real-timely according to  $\Delta_{qr}$ ,  $\Delta_{dr}$  variation. The fuzzy theory can be adopted to realize variation of  $K_{qr}$ ,  $K_{dr}$  in the light of the experiences of experts.

Take  $K_{qr}$  for example and it is similar to  $K_{dr}$ . There are two fuzzy rule:

$$\text{If } s_{qr} \dot{s}_{qr} > 0, \text{ then } K_{qr} \text{ should be increased} \quad (19)$$

$$\text{If } s_{qr} \dot{s}_{qr} < 0, \text{ then } K_{qr} \text{ should be decreased} \quad (20)$$

Fuzzy system about the relation between  $s_{qr} \dot{s}_{qr}$  and  $K_{qr}$  can be designed with respect to (19), (20). The fuzzy set is defined as:

$$\begin{aligned} s_{qr} \dot{s}_{qr} &= \{\text{NB NM ZO PM PB}\} \\ \Delta K_{qr} &= \{\text{NB NM ZO PM PB}\} \end{aligned}$$

Where NB is negative big, NM is negative middle, ZO is zero, PM is positive middle, PB is positive big.

The fuzzy rules are described as:

R1: IF  $s_{qr} \dot{s}_{qr}$  is PB THEN  $\Delta K_{qr}$  is PB.

R2: IF  $s_{qr} \dot{s}_{qr}$  is PM THEN  $\Delta K_{qr}$  is PM.

R3: IF  $s_{qr} \dot{s}_{qr}$  is ZO THEN  $\Delta K_{qr}$  is ZO.

R4: IF  $s_{qr} \dot{s}_{qr}$  is NM THEN  $\Delta K_{qr}$  is NM.

R5: IF  $s_{qr} \dot{s}_{qr}$  is NB THEN  $\Delta K_{qr}$  is NB.

The integral of  $\Delta K_{qr}$  is employed to estimate upper bound of  $K_{qr}$ .

$$\hat{K}_{qr} = G_1 \int_0^t \Delta K_{qr} dt \quad (21)$$

Where  $G_1$  is proportionality coefficient which is determined according to experience.

Then the last fuzzy sliding mode control law is as formula (23).

$$\begin{cases} u_{qr} = -g_1^{-1}(t, i_{qr}, i_{dr}, \omega_{rm}) \left( f_1(t, i_{qr}, i_{dr}, \omega_{rm}) + \hat{K}_{qr} \text{sign}(s_1) \right) \\ u_{dr} = -g_2^{-1}(t, i_{qr}, i_{dr}, \omega_{rm}) \left( f_2(t, i_{qr}, i_{dr}, \omega_{rm}) + \hat{K}_{dr} \text{sign}(s_2) \right) \end{cases} \quad (22)$$

#### 4. Simulation Results

To assess the designed controllers under realistic conditions, Two tests were conducted using a full-order model of the WECS including both the mechanical and the electric dynamics, together with uncertainties and disturbances. The fifth-order set of differential equations used in these simulations to model the WECS is detailed as follow.  $U_s = 380V$ ,  $\omega_s = 2\pi 60 \text{ rad/s}$ ,  $P_r = 50HP$ ,  $p = 2$ ,  $R_s = 0.082\Omega$ ,  $R_r = 0.228\Omega$ ,  $L_s = 0.0355H$ ,  $L_r = 0.0355H$ ,  $L_m = 0.0357H$ ,  $\rho = 1.224 \text{ kg/m}^3$ ,  $J = 3.662 \text{ kgm}^2$ ,  $B_l = 7.3m$ ,  $k_{gb} = 25$ ,  $C_{p\max} = 0.4$ ,  $\lambda_{opt} = 7.5$ ,  $c_1 = 9.5446$ ,  $c_2 = 12$ ,  $c_3 = 20$ .

In addition, external disturbances and parameters variation such as variations in the electric resistances and in the electromagnetic inductances was taken into consideration up to 8% of their rated values, and in the grid voltage and frequency up to 8% and 2% of their rated values respectively.

The values of the parameters for the controllers is finely adjusted with the aid of deep analysis of the system and realtime simulations, and the final choices are the following:  $\eta_{qr} = 5$ ,  $\eta_{dr} = 2$ ,  $G_1 = 1625$ ,  $G_2 = 382$ .

Mathematical formulas are utilized to describe the variation of the wind speed [11], and built two different wind speed models.

**4.1. Fitful Wind**

The mathematical formula to build the model of the fitful wind is described as equation (23). In this work, the base wind speed is 5m/s. The start-up time and variation cycle are 3s and 5s, respectively. The intensity of the fitful wind is 5m/s. The speed variation of the fitful wind is shown in Figure 4.

$$v = \begin{cases} t_b, & t < t_1 \\ t_b + 2.5(1 - \cos 2\pi(t/t_2 - t_1/t_2)), & t_1 \leq t \leq t_1 + t_2 \\ t_b, & t > t_1 + t_2 \end{cases} \quad (23)$$

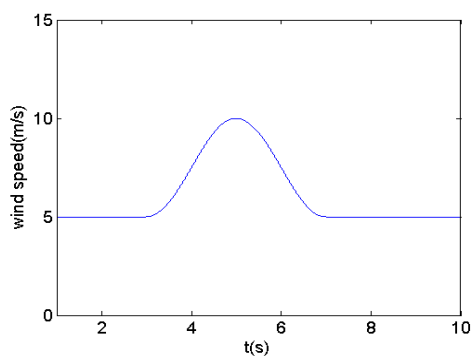


Figure 4. Speed Variation of Filful Wind

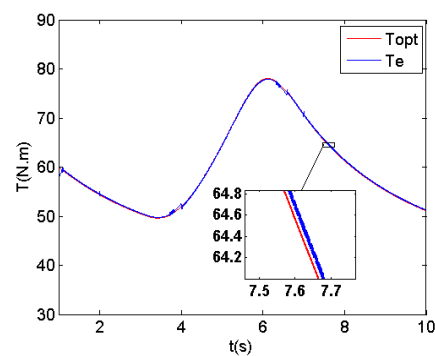


Figure 5. Electrical Torque and Torque Reference

The electrical resistant torque of the generator  $T_e$  and the torque reference being tracked,  $T_{opt}$  are depicted in Figure 5. The overlapping of both curves indicates the accomplishment of the first sliding objective. Figure 6 presents the temporal variations of the stator reactive power, Q, and of the reactive power reference, Qref. One curve is exactly over the other, showing the successful achievement of the second objective. Figure 7 presents the control inputs, the rotor voltages uqr(upper box), and udr(lower box), It is important to highlight the smoothness of the control signals.

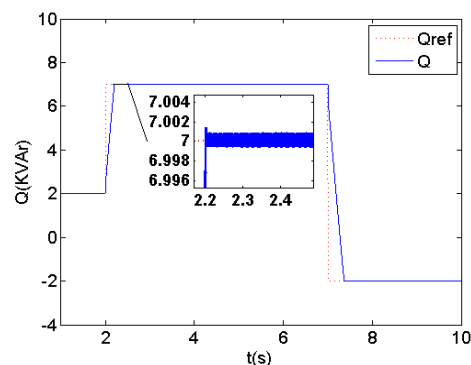


Figure 6. Reactive Stator Power and its Reference

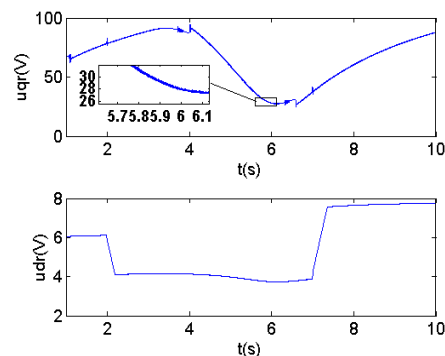


Figure 7. Control Voltages uqr and udr

### 4.2. Random Wind

The mathematical formula to build the model of the random wind is described as equation (24). The base wind velocity is 10m/s. The intensity of random wind is 3m/s. The speed variation of the fitful wind is shown in Figure 8.

$$v = v_s \text{unifrnd}(-0.5, 0.5) \cos(\omega t + \vartheta) + v_b \tag{24}$$

Where  $v_s$  is intensity of random wind(m/s),  $\text{unifrnd}(-0.5, 0.5)$  is random sampling value(range between -0.5 to 0.5) .

Figure 9 indicates reactive power tracking curve is good when wind speed changes randomly. The electrical torque optimization curve is described in Figure10. After the initial response time it can track the optimal torque which is determined by wind speed. The control voltage components  $u_{qr}$ ,  $u_{dr}$  are depicted in Figure 11 and its partial enlarged is Figure 12 from which we can see the chattering is small enough for satisfying relevant electrical codes.

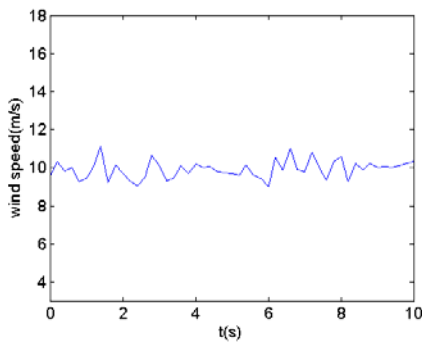


Figure 8. Speed Variation of Filful Wind

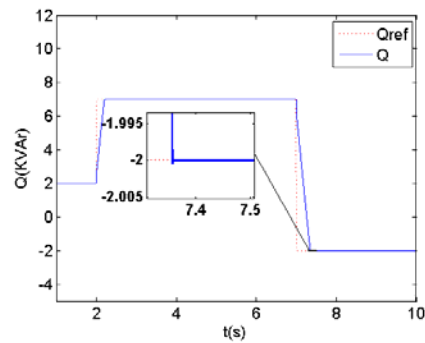


Figure 9. Reactive Power and its Reference

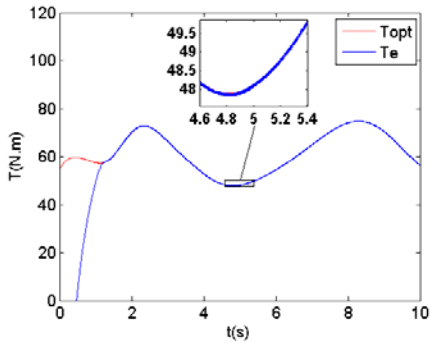


Figure 10. Electrical Torque and Torque Reference

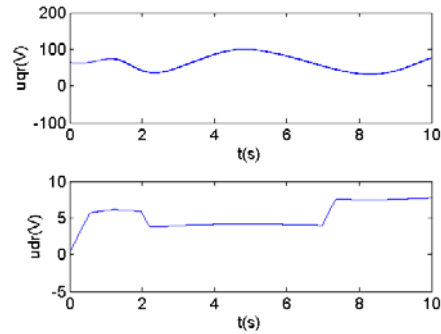


Figure 11. Control Voltages  $u_{qr}$  and  $u_{dr}$

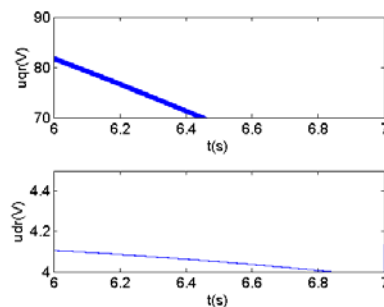


Figure 12. Partial Enlarged of Control Voltages  $u_{qr}$  and  $u_{dr}$

## 5. Conclusion

Two main objectives of a grid-connected variable-speed WECS were completed by sliding mode control strategy with fuzzy switching gain adjustment. Two wind speed models are used according to the characteristics of wind that wind turbine may meet with. The resulting controller was tested afterward through extensive simulations using a realistic and disturbed full-order model. It was shown that the control objectives were successfully attained, performing robustly despite the considered disturbances and uncertainties, and the increase in the order of the system. In order to satisfy latest electrical codes, next we will study fuzzy sliding mode control for WECS under harmonics grid voltage and little imbalances conditions

## Acknowledgements

This work is partially supported by National Natural Science Foundation of China under Grant 60974051, Grant 61273144, and in part by the Natural Science Foundation of Beijing under Grant 4122071 to Xiangjie Liu and A Project of Shandong Province Higher Educational Science and Technology Program under Grant J12LN29 and Shandong Provincial Natural Science Foundation under Grant ZR2013EEL014, ZR2013ZEM006 to Yaozhen Han, Hairong Xiao and Shandong Province Transportation Innovation Program (No. 2012-33) to Hu guanshan.

## References

- [1] GWEC. Global wind energy outlook. Global Wind Energy Council Report. Available: <http://www.gwec.net/>
- [2] Beltran, Brice, Tarek Ahmed-Ali, Mohamed Benbouzid. High-order sliding-mode control of variable-speed wind turbines. *Industrial Electronics, IEEE Transactions on*. 2009; 56(9): 3314-3321.
- [3] H Simpson, *Dumb Robots*, 3rd ed., Springfield: UOS Press, 2004, pp.6-9.
- [4] De Battista, Hernn, Ricardo J Mantz. Dynamical variable structure controller for power regulation of wind energy conversion systems. *Energy Conversion, IEEE Transactions on*. 2004; 19(4): 756-763.
- [5] Zhang Xianyong, Wu Jie, Yang Junjian, et al. Decoupled power control with sliding mode for brussless doubly-fed machine. *Ac Tae Ner Giae Solaris Sinica*. 2007; 128(1): 68-73. (In Chinese)
- [6] Hu J, Nian H, Hu B, He Y, Zhu ZQ. Direct active and reactive power regulation of DFIG using sliding-mode control approach. *Energy Conversion, IEEE Transactions on*. 2010; 25(4): 1028-1039.
- [7] Valenciaga F, CA Evangelista. 2-sliding active and reactive power control of a wind energy conversion system. *Control Theory & Applications, IET*. 2010; 4(11): 2479-2490.
- [8] C Evangelista, P Puleston, F Valenciaga, LM Fridman. Lyapunov-Designed Super-Twisting Sliding Mode Control for Wind Energy Conversion Optimization. *IEEE Transactions on industrial electronics*. 2013; 60(2): 538-545.
- [9] Abdullah MA, Yatim AHM, Tan CW, et al. A review of maximum power point tracking algorithms for wind energy systems. *Renewable and Sustainable Energy Reviews*. 2012; 16(5): 3220-3227.
- [10] Chen SZ, Cheung NC, Wong KC, et al. Integral sliding-mode direct torque control of doubly-fed induction generators under unbalanced grid voltage. *Energy Conversion, IEEE Transactions on*. 2010; 25(2): 356-368.
- [11] Beltran B, El Hachemi Benbouzid M, Ahmed-Ali T. Second-order sliding mode control of a doubly fed induction generator driven wind turbine. *Energy Conversion, IEEE Transactions on*. 2012; 27(2): 261-269.
- [12] Chen HC, Chen PH. Active and Reactive Power Control of a Doubly Fed Induction Generator. *Applied Mathematics & Information Sciences*. 2014; 8(1L): 117-124.